THE JOURNAL OF PHYSICAL CHEMISTRY A LETTERS

2009, *113,* 7707–7713
Published on Web 06/16/2009

Direct Emission of I_2 Molecule and IO Radical from the Heterogeneous Reactions of Gaseous Ozone with Aqueous Potassium Iodide Solution

Yosuke Sakamoto, Akihiro Yabushita, and Masahiro Kawasaki*

Department of Molecular Engineering, Kyoto University, Kyoto 615-8510, Japan

Shinichi Enami

W. M. Keck Laboratories, California Institute of Technology, Pasadena, California 91125

Received: April 16, 2009; Revised Manuscript Received: May 21, 2009

Recent studies indicated that gaseous halogens mediate key tropospheric chemical processes. The inclusion of halogen-ozone chemistry in atmospheric box models actually closes the ~50% gap between estimated and measured ozone losses in the marine boundary layer. The additional source of gaseous halogens is deemed to involve previously unaccounted for reactions of O_3(g) with sea surface water and marine aerosols. Here, we report that molecular iodine, I_2(g), and iodine monoxide radical, IO(g), are released ($[I_2(g)] > 100[IO(g)]$) during the heterogeneous reaction of gaseous ozone, O_3(g), with aqueous potassium iodide, KI(aq). It was found that (1) the amounts of I_2(g) and IO(g) produced are directly proportional to [KI(aq)] up to 5 mM and (2) IO(g) yields are independent of bulk pH between 2 and 11, whereas I_2(g) production is markedly enhanced at pH < 4. We propose that O_3(g) reacts with I^- at the air/water interface to produce I_2(g) and IO(g) *via* HOI and $IOOO^-$ intermediates, respectively.

Introduction

Recent field observations in the marine boundary layer (MBL), atmospheric box models, and laboratory experiments have revealed that activated halogens play various essential roles in the global environment. Halogens deplete tropospheric ozone, perturb the HO_x/NO_x cycle, and generate cloud condensation nuclei (CCN), thereby influencing climate change.[1−4] Unexpectedly high concentrations of the iodine monoxide radical, IO(g) (up to 5−10 times higher than previous measurements) were recently determined over the ocean.[5,6] The detection of IO(g) and OIO(g) at nighttime suggests the existence of a dark source.[4,7] Significantly, IO(g) was detected across the tropical Atlantic ocean, i.e., far away from biogenic coastal sources.[8] These observations suggest a hitherto unknown but ubiquitous IO(g) source, which could significantly affect the global O_3 budget. Enhanced halogen-ozone chemistry is actually able to correct atmospheric box models that underestimated the extent of tropospheric ozone loss by 50%.[8]

It is generally believed that the primary sources of reactive iodine compounds in the MBL are biogenic I_2(g)[9−11] and alkyl iodide emissions.[12] I_2(g) is rapidly photolyzed into I atoms, which are rapidly oxidized to IO(g).[9] Alkyl iodides are photolyzed and/or oxidized by OH, Cl, and NO_3, ultimately leading to IO(g).[2,13−16] Recent field measurements show, however, that atmospheric box models based on biogenic iodine emissions cannot account for the observed levels of gas-phase iodine species, suggesting the existence of additional sources of reactive iodine over and across the oceans.[8]

The observed ozone deposition velocities over seawater range from 0.01 to 0.12 cm s^{-1}.[17−20] Garland and co-workers first proposed that halides at the sea surface can enhance O_3(g) uptake,[21] and experimentally demonstrated that I_2(g) is emitted even in the absence of biogenic activity.[22] More recently, it has been reported that I^- in the sea surface microsublayer enhances O_3(g) uptake, even though I^- concentrations in bulk seawater are extremely low ($[I^-]/[Cl^-] \sim 10^{-6}$).[23,24] Fine sea salt aerosol particles, which are significantly enriched in I^- relative to seawater (by 2−4 orders of magnitude),[25−28] react with O_3(g) to release photoactive inorganic halogen compounds, such as Br_2, into the MBL.[29] Brown et al. demonstrated that solid potassium iodide, KI(s), reacts with O_3(g) much faster than KBr(s) to produce KIO_3(s).[30−32] These results imply that I^- at both seawater and dehydrated/aqueous aerosol interfaces may mediate or catalyze gaseous reactive halogen production in the MBL.

Previous reports have suggested that the ozonation of aqueous aerosols containing I^- occurs primarily at the air/water interface.[29,33,34] The gas/liquid interface is a unique media that should be distinguished from the gas or liquid phases.[35−39] For example, I^- is more abundant at the air/water interface than in the bulk phase, in contrast with Cl^-.[40,41] Furthermore, surface-specific intermediates, which have not been previously detected in homogeneous reactions, have been recently identified.[36,42,43] Finlayson-Pitts and co-workers proposed that Br^- at the air/aerosol interface is converted by O_3(g) to a surface-specific $BrOOO^-$ intermediate, which ultimately yields Br_2(g).[44] It is apparent that further studies of rates and mechanisms of reactions at air/water interfaces are required to establish their possible relevance to atmospheric chemistry. Here, we report the detection of I_2(g) and IO(g) during the reaction of O_3(g)

* To whom correspondence should be addressed. E-mail: kawasaki@moleng.kyoto-u.ac.jp.

10.1021/jp903486u CCC: $40.75

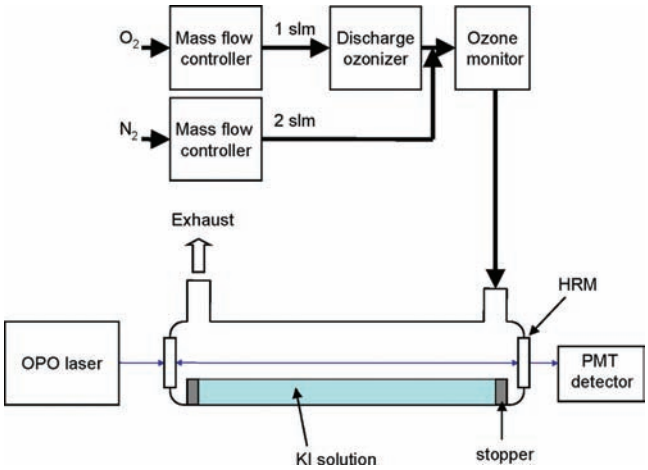

Figure 1. Schematic diagram of the present experimental setup combined with a CRDS and a gas/liquid interaction cell. HRM and PMT stand for high reflective mirror and photomultiplier tube, respectively. Synthetic resin putties are used for a solution stopper.

with aqueous KI(aq) in the dark by cavity ring-down spectroscopy (CRDS).[45−47]

Experimental Section

Figure 1 shows a schematic diagram of the experimental setup. The principle of CRDS and pertinent experimental details are presented in the Supporting Information and in previous publications.[48−50] O_3(g) was produced by 1 slm (standard liter per minute) O_2 flow through a high pressure discharge ozonizer and monitored by UV absorption by a 253.7 nm Hg lamp prior to the gas/liquid interaction cell. Gas flow rates were controlled by mass flow controllers, and the total flow rate was maintained at 3 slm. The concentrations of O_3(g) were in the range from 4.8×10^{13} to 7.3×10^{15} molecules cm^{-3} (2−298 ppmv). At O_3(g) concentrations greater than 1.0×10^{16} molecules cm^{-3}, aerosol formation from iodine oxides, I_nO_m,[51,52] was observed. To reduce the complication, [O_3(g)] was kept below 7.3×10^{15} molecules cm^{-3}, so that no aerosols were formed. The product concentrations were monitored with an OPO laser (Spectra-Physics, MOPO-SL, spectral resolution 0.2 cm^{-1}) at 435.6 nm for the IO(g) band head of the $A^2\Pi_{3/2} \leftarrow X^2\ \Pi_{3/2}$ ($v' = 3$, $v'' = 0$) transition. The absorption cross section of IO(g) at 435.63 nm was previously measured to be 5.9×10^{-17} cm^2 molecule^{-1} with the same wavelength resolution.[53] The IO(g) signal baseline was taken at 435.0 nm, a region in which there was no IO(g) absorption. [I_2(g)] was calibrated by introducing a concentration-known I_2(g) into the reaction cell with spectral fitting at 430−455 nm for the B−X band of I_2(g).[54] The I_2(g) absorption spectra were also measured at 532−540 nm. The observed IO(g) and I_2(g) concentrations in the present experiments were (0.03 − 4.0) $\times 10^{11}$ and (0.02 − 1.1) $\times 10^{14}$ molecules cm^{-3}, respectively.

The gas/liquid interaction cell consisted of a Pyrex glass container (21 or 96 mm i.d. and 60 cm length) fully covered with aluminum foil. The cell was maintained at 100 Torr by means of a rotary pump, a mechanical booster pump, and a N_2(l) trap in tandem, and monitored by an absolute pressure gauge. Since there was no appreciable difference in the results between the 21 and 96 mm reaction cells, all experiments were conducted at room temperature with the 21 mm cell. KI(aq) solution (0.01−50 mM and 50 mL) was filled 0.8 ± 0.1 cm above the bottom of the reaction cell (see Figure 1). The CRDS detection region is 2 mm above the solution surface. A slow flow of nitrogen gas (0.05 slm) was introduced at the ends of the ring-down cavity, close to the mirrors to minimize mirror deterioration caused by exposure to the reactants and products in the cell. The total flow rate was adjusted to 3 slm so that the gas in the cell was completely replaced within a 0.70 s time interval. Hence, the average contact time of O_3(g) with the KI(aq) solution was ∼0.70 s. To minimize possible secondary reactions, a freshly prepared solution was used for the measurement of each data point. The present application of CRDS enabled us to monitor primary gaseous products released from the reaction of O_3(g) with KI(aq) solutions with an adequate wavelength resolution and sensitivity in less than 1 s. Control experiments confirmed that dark heterogeneous reactions are exclusively responsible for I_2(g) and IO(g) production. See the Supporting Information for further details.

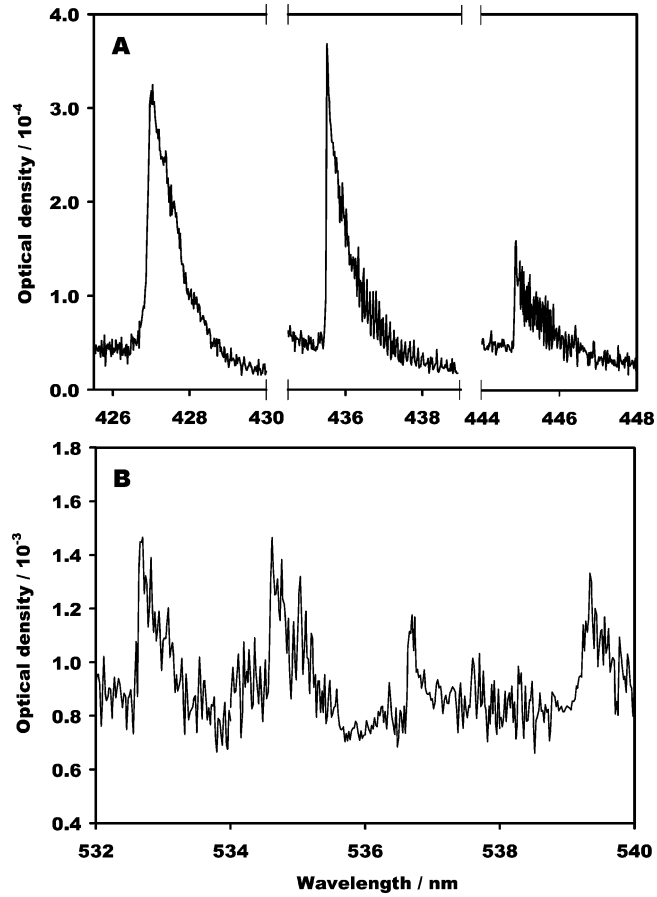

Figure 2. CRD spectra of gaseous IO (A) and I_2 (B) formed during the reaction of 7.3×10^{15} and 1.3×10^{16} molecules cm^{-3} O_3(g), respectively, with 5 mM KI solution at 100 Torr and at room temperature. The high [O_3(g)] for I_2 spectra was used for clarification of the spectrum, but other measurements were performed below 7.3×10^{15} molecules cm^{-3}.

Results

Figure 2 shows typical CRD spectra for IO(g) and I_2(g) during O_3(g) flow over the KI(aq) solution. We verified that neither absorption nor scattering signals appeared within the 420−450 and 530−540 nm detection ranges in the absence of O_3(g). There was no difference of the IO(g) and I_2(g) yields between NaI(aq) and KI(aq) solution (within 2%) because K^+ and Na^+ cations do not play a role in the interfacial reaction, which is consistent with the previous reports on the ozonolysis of NaI(s) and KI(s).[30−32] These results suggest that IO(g) and I_2(g) are produced from the reaction of O_3(g) with I^-(aq).

BrO(g) and Br_2(g) were not observed during the exposure of 2.4×10^{16} molecules cm^{-3} O_3(g) to a 50 mM KBr(aq) solution. Under the present conditions, the limit value of the detection is 2.7×10^{11} molecules cm^{-3} for Br_2(g) and 1.1×10^{11} molecules cm^{-3} for BrO(g). These results are consistent with the fact that the reaction rate constant of Br^-(aq) + O_3(aq), 248 M^{-1} s^{-1}, in the aqueous phase is 5×10^6 times lower than that of I^-(aq) + O_3(aq), 1.2×10^9 M^{-1} s^{-1}.[55] The lower air/water interface affinity of Br^- as compared to I^- will also lower its reaction probability.[40,41] The inertness of Br^-(aq) toward O_3(g) is consistent with previous studies.[29]

Other possible IO(g) sources were considered. For example, IO(g) could arise from the I_2(g) + O_3(g) reaction.[56] However, from the reported rate constant, $k = 4.3 \times 10^{-18}$ cm^3 $molecule^{-1}$ s^{-1} at 300 K[56] and [O_3(g)] $\sim 7.3 \times 10^{15}$ molecules cm^{-3}, the maximum concentrations used in the present study, the estimated reaction half-life is ~30 s, which is ~45 times longer than the present reaction time window, 0.70 s. Thus, the gaseous reaction of I_2(g) + O_3(g) is too slow to explain the formation of IO(g) in our system. Furthermore, a saturated aqueous iodine I_2(aq) solution in 50 mM KI (aq) did not enhance the total IO(g) yields even though $\sim 10^{14}$ molecules cm^{-3} I_2(g) is present before/after ozonation due to the evaporation. The ozonolysis of saturated I_2(aq) solution also did not produce any IO(g). We also confirmed that no IO(g) was formed from dry KI(s) that were fully bedded in the cell and exposed up to 7.5×10^{15} molecules cm^{-3} O_3(g). The results on KI(s) are consistent with previous reports on the ozonation of KI(s), which predominantly produced KIO_3(s).[30−32] Thus, no significant IO(g) is formed by ozonation of I_2(g/aq) and KI(s) under the present conditions. These experimental results therefore indicate that I^-(aq) is required to produce IO(g) in our setup. The results also suggest that IO(g) is produced directly from the reaction of O_3(g) + I^-(aq); however, other IO(g) production mechanisms involving the reaction of O_3(g) with product(s) from the reaction O_3(g) with I^-(aq) cannot be ruled out.

Figure 3 shows the IO(g) and I_2(g) formation as a function of [O_3(g)] at [KI(aq)] = 5 mM. The solid lines are the fitting curves to be used as eye guides. [I_2(g)] plateaus at [O_3(g)] ~ 1.0×10^{15} molecules cm^{-3}, while [IO(g)] plateaus later at [O_3(g)] ~ 5.0×10^{15} molecules cm^{-3}. The [IO(g)]/[I_2(g)] ratio is plotted as a function of [O_3(g)] in Figure 3C, and has a positive [O_3(g)] dependence. This behavior implies that the IO(g) and I_2(g) formation mechanisms involve different pathways and stoichiometries (see below). Figure 4 shows the [IO(g)] and [I_2(g)] as a function of [I^-(aq)] when [O_3(g)] = 7.3×10^{15} molecules cm^{-3}. Both products plateau when [I^-(aq)] > 5 mM, likely due to the mass transfer limitations. That is, the equilibrium between reactions and diffusion from the bulk was established at [I^-(aq)] > 5 mM when [O_3(g)] = 7.3×10^{15} molecules cm^{-3}.

The effective uptake coefficient, γ_{eff}, for O_3(g) on the KI(aq) solution was obtained from the difference between inflow and outflow [O_3(g)] (see the Supporting Information for details). γ_{eff} decreased with increasing [O_3(g)] from 1.7×10^{-4} to 0.8×10^{-4}, leveling off at higher [O_3(g)], as shown in Figure 5A. The observed γ_{eff} is well fitted by a Langmuir−Hinshelwood mechanism rather than an Eley−Rideal mechanism, which is consistent with a number of recent results of O_3(g) uptake.[57−69] γ_{eff} increased with increasing [I^-] from 0 to 50 mM, reaching a plateau at higher [I^-], as shown in Figure 5B. A fitting curve is obtained from a Langmuir−Hinshelwood mechanism (see the Supporting Information for details). The observed γ_{eff} vs [O_3(g)] plot correlates with IO(g)/I_2(g) yields as functions of [O_3(g)] (cf. Figure 3).

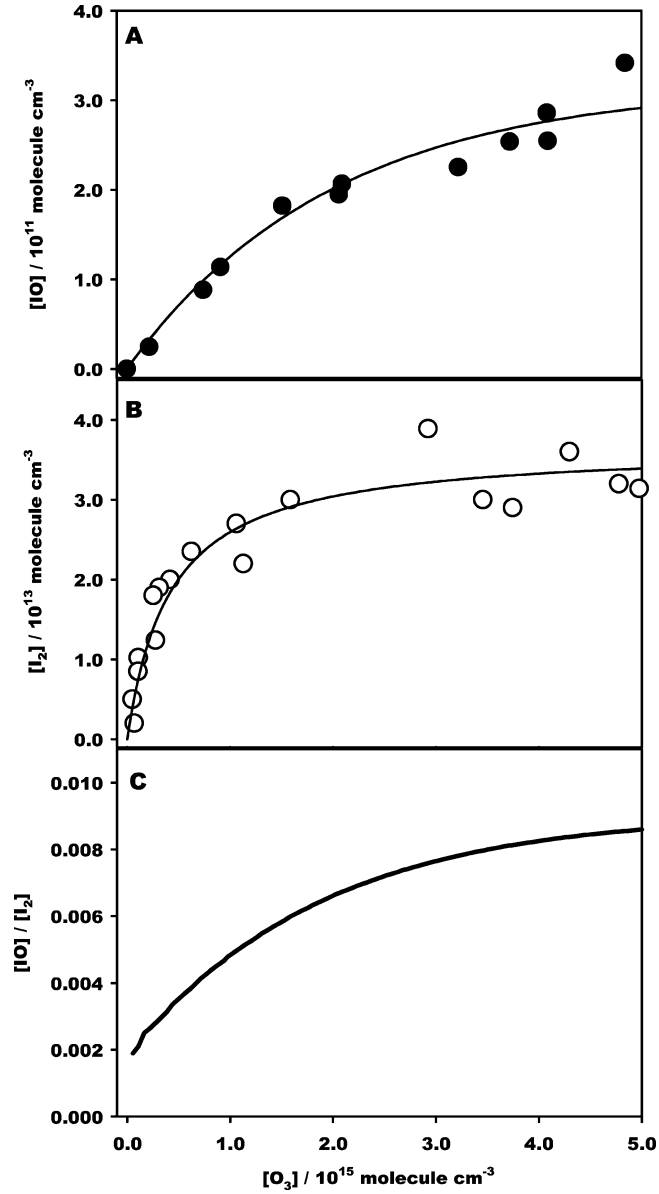

Figure 3. [IO(g)] (A) and [I_2(g)] (B) formed during the reaction of O_3(g) with 5 mM KI(aq) solution as a function of [O_3(g)]. Every plot has an uncertainty ~10% for IO and ~15% for I_2. (C) The [IO(g)]/[I_2(g)] ratio plotted as a function of [O_3(g)] at [KI(aq)] = 5 mM obtained from the fitting curves of parts A and B.

Figure 6 shows the IO(g) and I_2(g) production dependence on the bulk aqueous KI(aq) solution pH between 2 and 13 during the reaction with O_3(g). There is a significant difference of the pH profiles between the IO(g) and I_2(g) formation. The IO(g) formation was independent of the bulk pH from 2 to 11, while I_2 production significantly decreased (by a factor of ~7) from pH 2 to 4 and then remained approximately constant from pH 4 to 11. The enhancement of the I_2(g) production below pH 4 may be the result of the reaction $H^+ + HOI + I^- \rightarrow I_2 + H_2O$. Above pH 11, both the IO(g) and I_2(g) production decrease significantly to levels below the limit of the detection. A couple of explanations will be evaluated. First, the interfacial I^- concentration may be decreased due to the competition for the surface sites with [OH^-] >10 mM, hindering the interfacial reaction rate of interfacial I^- with O_3(g). A second explanation could be that, at pH > 11, IO^- is the dominant species (HOI ⇄

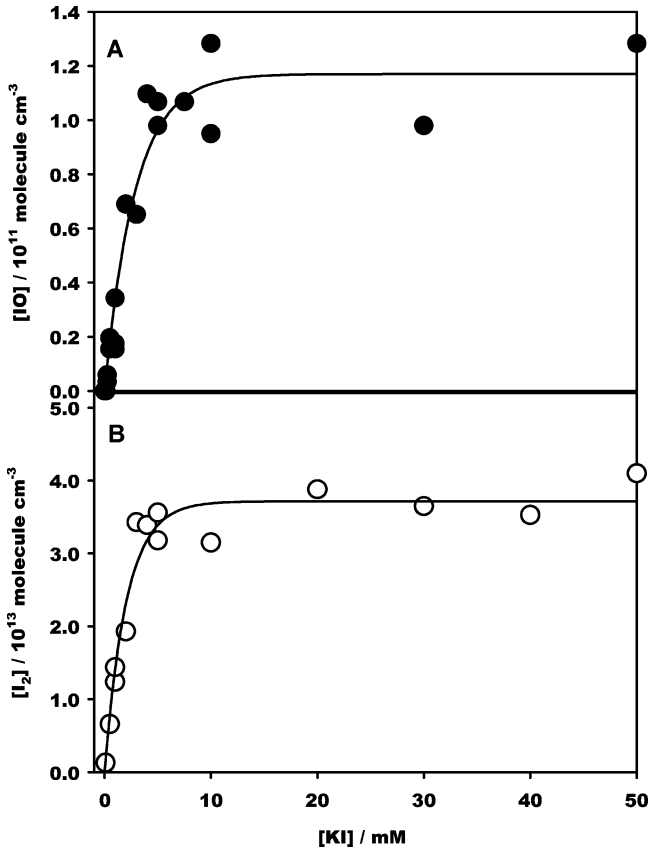

Figure 4. [IO(g)] (A) and [I_2(g)] (B) formed during the reaction of 7.3×10^{15} molecules cm^{-3} O_3(g) as a function of [KI(aq)]. Every plot has an uncertainty of ~10% for IO and ~15% for I_2.

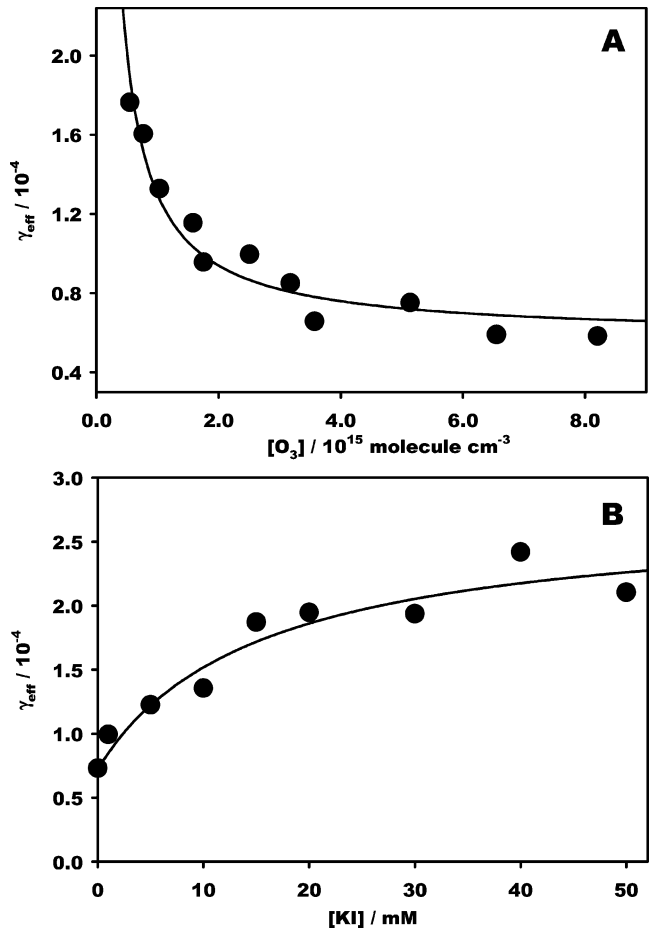

Figure 5. (A) Effective uptake coefficient, γ_{eff}, of O_3(g) on 5 mM KI(aq) solution as a function of [O_3(g)]. (B) Effective uptake coefficient of 1.4×10^{15} molecules cm^{-3} O_3(g) as a function of [KI(aq)]. Every plot has an ~30% uncertainty.

$H^+ + IO^-$; p$K_a = 10.8$) and has a different reactivity than HOI. For example, unlike HOI, IO^- may not react with I^- to yield I_2.

The apparent bulk pH effects on the product formation exclude the possibility that the observed IO(g) is generated from the gas-phase reaction of I_2 with O_3.[56] We also monitored the pH change of 5 mM KI(aq) after 5 min of 5.0×10^{15} molecules cm^{-3} ozonation. The pH was observed to increase from 7.0 to 11.3. The significant increase in pH (decrease in [H^+]) can be explained by the reaction mechanism proposed below.

Discussion

From the Henry's law constant for O_3(g) in water at 298 K, $H = 0.012$ M atm^{-1}, we calculate $[O_3(aq)]_{sat} = \sim 20$ μM under $[O_3(g)] = 5 \times 10^{15}$ molecules cm^{-3}. From the calculation to derive the diffusion depth[36] with the 0.7 s reaction time and a diffusion coefficient of 10^{-5} cm^2 s^{-1}, I^- only in the top ~50 μm of aqueous solution (in 8 mm depth) will be available for the reaction with dissolved O_3. Furthermore, I^- preferentially partitions to the air/water interface.[38−40] Also, the reaction of I^-(aq) with O_3(aq) is diffusion controlled with $k = 1.2 \times 10^9$ M^{-1} s^{-1}.[55] Considering these facts, it may be reasonable to assume that the reaction proceeds predominantly at the air/water interface rather than in the bulk phase.

Enami et al. showed that the reaction of I^- at the air/water interface of microdroplets with a ppmv level of O_3(g) can produce triiodide, I_3^-(aq) (in the equilibrium between I^-(aq) and I_2(aq)), and iodate, IO_3^-(aq), in a short reaction time of ~1 ms.[29] The observation of I_2(g) evolution agrees with the reported I_3^- formation.[29] The initial ozonation of I^- produces a hypoiodous acid intermediate (eqs 1, 2a, and 3), with a pK_a of 10.8. HOI can subsequently react with another I^-(aq), eq 4, to produce molecular iodine, I_2(aq). The produced I_2(aq) will either partition to the gas phase, eq 5, or complex with I^-(aq), to produce triiodide, eq 6.

$$I^-(aq) + O_3(g \text{ or interface}) \rightarrow IOOO^-(\text{interface}) \quad (1)$$

$$IOOO^-(\text{interface}) \rightarrow IO^-(aq) + O_2(aq) \quad (2a)$$

$$IO^-(aq) + H^+ \rightleftarrows HOI(aq) \quad (pK_a = 10.8) \quad (3)$$

$$HOI(aq) + I^-(aq) + H^+ \rightleftarrows I_2(aq) + H_2O \quad (4)$$

$$I_2(aq) \rightarrow I_2(g) \quad (5)$$

$$I_2(aq) + I^-(aq) \rightleftarrows I_3^-(aq) \quad (6)$$

$$HOI/IO^-(aq) + 2O_3(aq) \rightarrow IO_3^-(aq) + 2O_2 + H^+ \quad (7)$$

O_3(g) may first dissolve in the air/water interface *via* a Langmuir−Hinshelwood mechanism (see Figure 5 and the

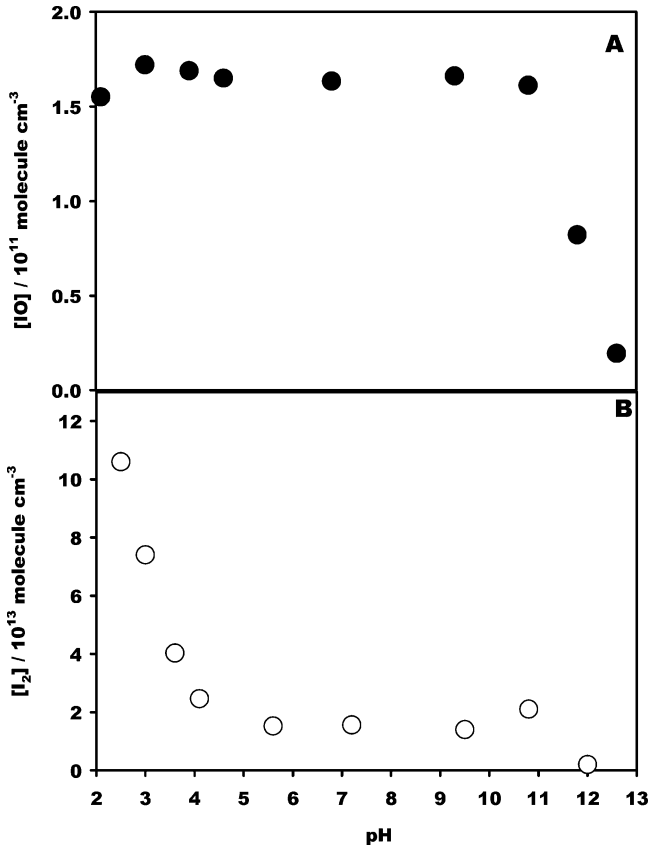

Figure 6. [IO(g)] (A) and [I_2(g)] (B) formed during the reaction of O_3(g) as a function of bulk pH. Every plot has an uncertainty of ~10% for IO and ~15% for I_2.

Supporting Information).[59] Here, we will propose the initial ozonation of I^-(aq) proceeds through a trioxide intermediate, $IOOO^-$(interface), which is assumed to have a similar structure and reactivity as the reported $BrOOO^-$ intermediate.[44,55] This unstable intermediate is different from the stable iodate, IO_3^- ($\Delta_f G°(IO_3^-(aq)) = -134.9$ kJ mol^{-1}).

An enhancement of I_2(g) formation when using acidic (pH < 4) KI(aq) is explained by reaction 4. The observation of the absence of I_2(g) formation from the ozonolysis of dried KI(s) is consistent with a reaction mechanism where H^+ is necessary to generate I_2. The observation of the significant pH increase from 7.0 to 11.3 during the ozonation also supports this mechanism.

A Dushman mechanism (eq 8) might also explain the present pH enhancement.[70,71]

$$IO_3^- + 5I^- + 6H^+ \rightarrow 3I_2 + 3H_2O \qquad (8)$$

However, under low pH conditions, the IO_3^-(aq) product is only expected to be a minor product compared with the I_2 product under the present high I^-(aq) conditions due to the fact that reaction 4 is faster than reaction 7. Thus, the Dushman mechanism itself cannot produce sizable I_2(g) in our experiments.

As far as we know, the direct formation of IO(g) from the heterogeneous reaction of I^-(aq) with O_3(g) has not been reported before. We have confirmed this overall reaction mechanism by attempting a number of control ozonation experiments. The reaction of O_3(g) with saturated I_2(aq) does not produce significant IO(g), which suggests that O_3(g) does not react with I_2 to produce IO(g) under the present conditions. The fact that IO(g) is emitted from the KI(aq) solution surface is inconsistent with the production of IO in bulk aqueous solution if one apply a diffusion-controlled rate constant of 1.5×10^9 M^{-1} s^{-1} for IO(aq) + IO(aq).[72] All IO(aq) would have been self-consumed and converted to I_2 and IO_3^- within 1 s. Therefore, O_3(g) or dissolved O_3(interface) reacts with I^-(aq) to produce $IOOO^-$(interface) and subsequently IO and HOI at the air/water interface rather than in the bulk. The produced IO(interface) is then rapidly emitted into the gas phase prior to consumption by reactions. Considering the absence of [H^+] effects over a pH range of 2−10, the IO formation is expected to occur shortly after the initial reaction step, eq 1. IO formation at the air/water interface could be explained by a number of unimolecular and/or bimolecular reactions involving the $IOOO^-$ intermediate, eqs 2b, 9, 10, and 11.

$$IOOO^- \rightarrow IO + O_2^- \qquad (2b)$$

$$IOOO^- + I^- \rightarrow \ \rightarrow IO + \text{products} \qquad (9)$$

$$IOOO^- + IOOO^- \rightarrow \ \rightarrow IO + \text{products} \qquad (10)$$

$$IOOO^- + HOI \rightarrow \ \rightarrow IO + \text{products} \qquad (11)$$

$$IO(aq) \rightarrow IO(g) \qquad (12)$$

Liu et al. theoretically reported that Br^-(aq) may form a stable $BrOOO^-$ intermediate during the reaction of Br^-(aq) with O_3(aq), which decomposes to yield $BrO^- + O_2$.[55] The O−O bond nearest to the bromine $BrO-OO^-$ is elongated to 2.033 Å in length and thus more likely to be broken, while the BrO bond is rather strong with a computed length of 1.813 Å.[55] As mentioned above, Br^- at the air/aerosol interface may react with O_3(g) to form a surface-specific $BrOOO^-$ intermediate, which further reacts to form Br_2(g).[44] Similarly, the fate of $IOOO^-$ will be favorably $IO^- + O_2$ from reaction 2a by way of thermochemical considerations, as it is very exothermic, but IO + O_2^- (eq 2b) might also be possible. Even if it occurred, its contribution would be minor because of the observed results which give a product ratio of [I_2(g)]/[IO(g)] > 100. In addition, thermodynamic data also imply this reaction will be unfavorable: $\Delta_f G°(I^-(aq)) = -51.7$,[73] $\Delta_f H°(O_3(g)) = 142.7$,[73] $\Delta_f H°(IO(g)) = 121.5$,[74] and $\Delta_f G°(O_2^-(aq)) = 31.8$[73] (kJ mol^{-1}). Thus, one may expect that the bimolecular reactions such as eqs 9−11 are more responsible for the IO formation than the unimolecular reaction, eq 2b. Theoretical calculations for the thermodynamic and kinetic data of the $IOOO^-$ intermediate are desirable. The proposed reaction mechanism is summarized in Scheme 1.

The present observation that [I_2(g)] > [IO(g)] may be explained by some effects other than the reaction pathways of $IOOO^-$ discussed above.

(1) The emissions of IO(g) and I_2(g) are largely controlled by the Henry's law constants. The values 3.0 for I_2 and 4.5×10^2 M atm^{-1} for HOI were reported, respectively.[72] Although the value for IO has not been determined yet, the same value for IO and HOI can be assumed.[72] If so, one can expect that I_2(g) is preferably in the gas phase rather than IO(g).

(2) Reactions of IO may occur in the gas phase or at the interface, since IO has a much greater reactivity than I_2. IO(g or interface) may have been consumed by the self-reaction or reactions with other species prior to reaching

SCHEME 1: Proposed Reaction Mechanism for the Formation of I_2(g) and IO(g) from the Interaction of O_3(g) with I^-(aq)

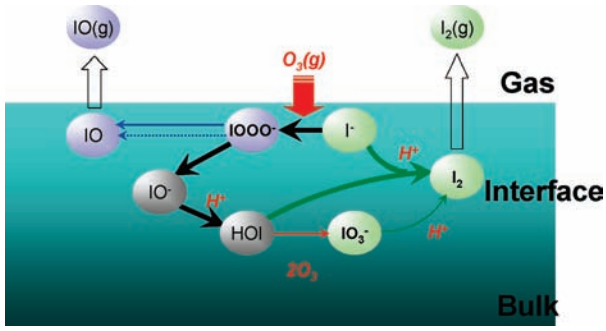

the detection region. Hence, the observed [IO(g)] at 2 mm above the aqueous surface may be significantly reduced from the initial concentration.

Atmospheric Implications

The present results for I_2(g) production are consistent with the work by Garland et al. demonstrating I_2(g) formation from both artificial and real seawater.[22] It is apparent that interaction of O_3(g) with 0.1−0.4 μM I^- at the seawater surface is a possible source of reactive iodine compounds. Recent field and modeling studies have revealed that I^- at the sea surface enhances O_3(g) uptake.[23,24] Thus, a large discrepancy in the observed O_3(g) deposition velocities over the seawater from 0.01 to 0.12 cm s^{-1} could be explained by I^-, one of the most active components in the seawater.[23,24] Here, we directly observe I_2 and IO as gas-phase products during the rapid O_3(g)−I^-(aq) interactions.

The present findings can be applied not only to the air/seawater interface but also to the air/aerosol interface. It should be emphasized that I^- in fine sea salt aerosol particles is significantly concentrated as compared to seawater by (2−4 orders of magnitude).[25−28] In actual aerosols, HOI(aq) would competitively react with O_3(g),[29] X^- (X = I, Br, Cl),[29] sulfur(IV),[34] and organic species.[75−77] The reaction of HOI with Br^-/Cl^- yields IBr/ICl, which could be emitted as IBr/ICl or Br_2/Cl_2 after subsequent processing in the gas phase.[29] At an iodine-enriched area such as Mace Head at the West sea of Ireland and Lilia at the French Atlantic Coast of Brittany,[12] strong I_2(g) emissions from the reaction of HOI(aq) with I^-(aq) initiated by I^-(aq) + O_3(g) at the air/aerosol interface would be expected. The reported Henry's law constants, $H = 3.0$ for I_2, 2.4 × 10 for IBr, and 1.1 × 10^2 M atm^{-1} for ICl[72] imply that a large fraction of I_2(g) emissions into the gas phase are more favorable than those of IBr(g)/ICl(g). Thus, whether sea salt aerosols release photoactive inorganic halogen compounds into the MBL or not is largely dependent on the actual compositions.[29] Here, we have shown that I_2(g) emissions from the O_3(g) + I^-(aq) reaction are enhanced up to 7 times at pH < 4 over those at pH 5−10, and that non-negligible amounts of IO(g) should be also emitted even at nighttime.

Acknowledgment. The authors appreciate Ms. S. Hayase for help with experiments. We greatly appreciate Dr. A. J. Colussi of California Institute of Technology and Dr. Chad. D. Vecitis of Yale University for valuable discussions. S.E. thanks the JSPS Research Fellowships for Young Scientists. This work is partly supported by a Grant-in-Aid from JSPS (#20245005).

Supporting Information Available: Experimental details. This material is available free of charge via the Internet at http://pubs.acs.org.

References and Notes

(1) von Glasow, R.; Crutzen, P. J., *Tropospheric Halogen Chemistry in Treatise on Geochemistry* ed. by Holland, H. D. Turekian, K. K. 2007.
(2) Carpenter, L. J. *Chem. Rev.* **2003**, *103*, 4953–4962.
(3) von Glasow, R. *Nature* **2008**, *453*, 1195–1196.
(4) Saiz-Lopez, A.; Plane, J. M. C. *Geophys. Res. Lett.* **2004**, *31*, L03111.
(5) Wada, R.; Beames, J. M.; Orr-Ewing, A. J. *J. Atmos. Chem.* **2007**, *58*, 69–87.
(6) Saiz-Lopez, A.; Mahajan, A. S.; Salmon, R. A.; Bauguitte, S. J. B.; Jones, A. E.; Roscoe, H. K.; Plane, J. M. C. *Science* **2007**, *317*, 348–351.
(7) Cainey, J. M.; Keywood, M.; Grose, M. R.; Krummel, P.; Galbally, I. E.; Johnston, P.; Gillett, R. W.; Meyer, M.; Fraser, P.; Steele, P.; Harvey, M.; Kreher, K.; Stein, T.; Ibrahim, O.; Ristovski, Z. D.; Johnson, G.; Fletcher, C. A.; Bigg, E. K.; Gras, J. L. *Environ. Chem.* **2007**, *4*, 143–150.
(8) Read, K. A.; Mahajan, A. S.; Carpenter, L. J.; Evans, M. J.; Faria, B. V. E.; Heard, D. E.; Hopkins, J. R.; Lee, J. D.; Moller, S. J.; Lewis, A. C.; Mendes, L.; McQuaid, J. B.; Oetjen, H.; Saiz-Lopez, A.; Pilling, M. J.; Plane, J. M. C. *Nature* **2008**, *453*, 1232–1235.
(9) Saiz-Lopez, A.; Plane, J. M. C.; McFiggans, G.; Williams, P. I.; Ball, S. M.; Bitter, M.; Jones, R. L.; Hongwei, C.; Hoffmann, T. *Atmos. Chem. Phys.* **2006**, *6*, 883–895.
(10) Küpper, F. C.; Carpenter, L. J.; McFiggans, G. B.; Palmer, C. J.; Waite, T. J.; Boneberg, E. M.; Woitsch, S.; Weiller, M.; Abela, R.; Grolimund, D.; Potin, P.; Butler, A.; Luther, G. W.; Kroneck, P. M. H.; Meyer-Klaucke, W.; Feiters, M. C. *Proc. Natl. Acad. Sci. U.S.A.* **2008**, *105*, 6954–6958.
(11) Dixneuf, S.; Ruth, A. A.; Vaughan, S.; Varma, R. M.; Orphal, J. *Atmos. Chem. Phys.* **2009**, *9*, 823–829.
(12) Peters, C.; Pechtl, S.; Stutz, J.; Hebestreit, K.; Honninger, G.; Heumann, K. G.; Schwarz, A.; Winterlik, J.; Platt, U. *Atmos. Chem. Phys.* **2005**, *5*, 3357–3375.
(13) Enami, S.; Yamanaka, T.; Hashimoto, S.; Kawasaki, M.; Tonokura, K.; Tachikawa, H. *Chem. Phys. Lett.* **2007**, *445*, 152–156.
(14) Cotter, E. S. N.; Canosa-Mas, C. E.; Manners, C. R.; Wayne, R. P.; Shallcross, D. E. *Atmos. Environ.* **2003**, *37*, 1125–1133.
(15) Nakano, Y.; Ishiwata, T.; Kawasaki, M. *J. Phys. Chem. A* **2005**, *109*, 6527–6531.
(16) Enami, S.; Hashimoto, S.; Kawasaki, M.; Nakano, Y.; Ishiwata, T.; Tonokura, K.; Wallington, T. J. *J. Phys. Chem. A* **2005**, *109*, 1587–1593.
(17) Gallagher, M. W.; Beswick, K. M.; Coe, H. *Q. J. R. Meteorol. Soc.* **2001**, *127*, 539–558.
(18) Lenschow, D. H.; Pearson, R.; Stankov, B. B. *J. Geophys. Res.-Oceans Atmos.* **1982**, *87*, 8833–8837.
(19) Galbally, I. E.; Roy, C. R. *Q. J. R. Meteorol. Soc.* **1980**, *106*, 599–620.
(20) Kawa, S. R.; Pearson, R. *J. Geophys. Res. -Atoms.* **1989**, *94*, 9809–9817.
(21) Garland, J. A.; Elzerman, A. W.; Penkett, S. A. *J. Geophys. Res.* **1980**, *85*, 7488–7492.
(22) Garland, J. A.; Curtis, H. *J. Geophys. Res.* **1981**, *86*, 3183–3186.
(23) Chang, W. N.; Heikes, B. G.; Lee, M. H. *Atmos. Environ.* **2004**, *38*, 1053–1059.
(24) Oh, I. B.; Byun, D. W.; Kim, H. C.; Kim, S.; Cameron, B. *Atmos. Environ.* **2008**, *42*, 4453–4466.
(25) Duce, R. A.; Wasson, J. T.; Winchester, J. W.; Burns, E. *J. Geophys. Res.* **1963**, *68*, 3943–3947.
(26) Seto, F. Y. B.; Duce, R. A. *J. Geophys. Res.* **1972**, *77*, 5339–5349.
(27) Duce, R. A.; Winchest, Jw; Vannahl, T. W. *J. Geophys. Res.* **1965**, *70*, 1775–1799.
(28) Martens, C. S.; Wesolows, J. J.; Harriss, R. C.; Kaifer, R. *J. Geophys. Res.* **1973**, *78*, 8778–8792.
(29) Enami, S.; Vecitis, C. D.; Cheng, J.; Hoffmann, M. R.; Colussi, A. J. *J. Phys. Chem. A* **2007**, *111*, 8749–8752.
(30) Brown, M. A.; Ashby, P. D.; Ogletree, D. F.; Salmeron, M.; Hemminger, J. C. *J. Phys. Chem. C* **2008**, *112*, 8110–8113.
(31) Brown, M. A.; Liu, Z.; Ashby, P. D.; Mehta, A.; Grimm, R. L.; Hemminger, J. C. *J. Phys. Chem. C* **2008**, *112*, 18287–18290.
(32) Brown, M. A.; Newberg, J. T.; Krisch, M. J.; Mun, B. S.; Hemminger, J. C. *J. Phys. Chem. C* **2008**, *112*, 5520–5525.
(33) Enami, S.; Vecitis, C. D.; Cheng, J.; Hoffmann, M. R.; Colussi, A. J. *J. Phys. Chem. A* **2007**, *111*, 13032–13037.
(34) Enami, S.; Vecitis, C. D.; Cheng, J.; Hoffmann, M. R.; Colussi, A. J. *Chem. Phys. Lett.* **2008**, *455*, 316–320.
(35) Buch, V.; Milet, A.; Vacha, R.; Jungwirth, P.; Devlin, J. P. *Proc. Natl. Acad. Sci. U. S. A.* **2007**, *104*, 7342–7347.
(36) Davidovits, P.; Kolb, C. E.; Williams, L. R.; Jayne, J. T.; Worsnop, D. R. *Chem. Rev.* **2006**, *106*, 1323–1354.
(37) Enami, S.; Hoffmann, M. R.; Colussi, A. J. *Proc. Acad. Natl. Sci. U.S.A.* **2008**, *105*, 7365–7369.

(38) Ghosal, S.; Hemminger, J. C.; Bluhm, H.; Mun, B. S.; Hebenstreit, E. L. D.; Ketteler, G.; Ogletree, D. F.; Requejo, F. G.; Salmeron, M. *Science* **2005**, *307*, 563–566.
(39) Jungwirth, P.; Tobias, D. J. *J. Phys. Chem. B* **2001**, *105*, 10468–10472.
(40) Cheng, J.; Vecitis, C. D.; Hoffmann, M. R.; Colussi, A. J. *J. Phys. Chem. B* **2006**, *110*, 25598–25602.
(41) Cheng, J.; Hoffmann, M. R.; Colussi, A. J. *J. Phys. Chem. B* **2008**, *112*, 7157–7161.
(42) Hu, J. H.; Shi, Q.; Davidovits, P.; Worsnop, D. R.; Zahniser, M. S.; Kolb, C. E. *J. Phys. Chem.* **1995**, *99*, 8768–8776.
(43) Knipping, E. M.; Lakin, M. J.; Foster, K. L.; Jungwirth, P.; Tobias, D. J.; Gerber, R. B.; Dabdub, D.; Finlayson-Pitts, B. J. *Science* **2000**, *288*, 301–306.
(44) Hunt, S. W.; Roeselova, M.; Wang, W.; Wingen, L. M.; Knipping, E. M.; Tobias, D. J.; Dabdub, D.; Finlayson-Pitts, B. J. *J. Phys. Chem. A* **2004**, *108*, 11559–11572.
(45) Okeefe, A.; Deacon, D. A. G. *Rev. Sci. Instrum.* **1988**, *59*, 2544–2551.
(46) Wheeler, M. D.; Newman, S. M.; Orr-Ewing, A. J.; Ashfold, M. N. R. *J. Chem. Soc.-Faraday Trans.* **1998**, *94*, 337–351.
(47) Yu, T.; Lin, M. C. *J. Am. Chem. Soc.* **1993**, *115*, 4371–4372.
(48) Ninomiya, Y.; Hashimoto, S.; Kawasaki, M.; Wallington, T. J. *Int. J. Chem. Kinet.* **2000**, *32*, 125–130.
(49) Enami, S.; Hoshino, Y.; Ito, Y.; Hashimoto, S.; Kawasaki, M.; Wallington, T. J. *J. Phys. Chem. A* **2006**, *110*, 3546–3551.
(50) Enami, S.; Ueda, J.; Nakano, Y.; Hashimoto, S.; Kawasaki, M. *J. Geophys. Res.* **2004**, 109.
(51) Burkholder, J. B.; Curtius, J.; Ravishankara, A. R.; Lovejoy, E. R. *Atmos. Chem. Phys.* **2004**, *4*, 19–34.
(52) Martin, J. C. G.; Spietz, P.; Burrows, J. P. *J. Phys. Chem. A* **2007**, *111*, 306–320.
(53) Nakano, Y.; Enami, S.; Nakamichi, S.; Aloisio, S.; Hashimoto, S.; Kawasaki, M. *J. Phys. Chem. A* **2003**, *107*, 6381–6387.
(54) Spietz, P.; Martin, J. C. G.; Burrows, J. P. *J. Photoch. Photobio. A* **2005**, *176*, 50–67.
(55) Liu, Q.; Schurter, L. M.; Muller, C. E.; Aloisio, S.; Francisco, J. S.; Margerum, D. W. *Inorg. Chem.* **2001**, *40*, 4436–4442.
(56) Vikis, A. C.; Macfarlane, R. *J. Phys. Chem.* **1985**, *89*, 812–815.
(57) Gonzalez-Labrada, E.; Schmidt, R.; DeWolf, C. E. *Phys. Chem. Chem. Phys.* **2007**, *9*, 5814–5821.
(58) Clifford, D.; Donaldson, D. J.; Brigante, M.; D'Anna, B.; George, C. *Environ. Sci. Technol.* **2008**, *42*, 1138–1143.
(59) McCabe, J.; Abbatt, J. P. D. *J. Phys. Chem. C* **2009**, *113*, 2120–2127.
(60) Ammann, M.; Poschl, U.; Rudich, Y. *Phys. Chem. Chem. Phys.* **2003**, *5*, 351–356.
(61) Chang, R. Y. W.; Sullivan, R. C.; Abbatt, J. P. D. *Geophys. Res. Lett.* **2005**, 32.
(62) Dubowski, Y.; Vieceli, J.; Tobias, D. J.; Gomez, A.; Lin, A.; Nizkorodov, S. A.; McIntire, T. M.; Finlayson-Pitts, B. J. *J. Phys. Chem. A* **2004**, *108*, 10473–10485.
(63) Hanisch, F.; Crowley, J. N. *Atmos. Chem. Phys.* **2003**, *3*, 119–130.
(64) Kahan, T. F.; Kwamena, N. O. A.; Donaldson, D. J. *Atmos. Environ.* **2006**, *40*, 3448–3459.
(65) Kwamena, N. O. A.; Staikova, M. G.; Donaldson, D. J.; George, I. J.; Abbatt, J. P. D. *J. Phys. Chem. A* **2007**, *111*, 11050–11058.
(66) Kwamena, N. O. A.; Thornton, J. A.; Abbatt, J. P. D. *J. Phys. Chem. A* **2004**, *108*, 11626–11634.
(67) McNeill, V. F.; Wolfe, G. M.; Thornton, J. A. *J. Phys. Chem. A* **2007**, *111*, 1073–1083.
(68) Mmereki, B. T.; Donaldson, D. J. *J. Phys. Chem. A* **2003**, *107*, 11038–11042.
(69) Sullivan, R. C.; Thornberry, T.; Abbatt, J. P. D. *Atmos. Chem. Phys.* **2004**, *4*, 1301–1310.
(70) Dushman, S. *J. Phys. Chem.* **1904**, *8*, 453–482.
(71) Schmitz, G. *Phys. Chem. Chem. Phys.* **1999**, *1*, 1909–1914.
(72) Vogt, R.; Sander, R.; Von Glasow, R.; Crutzen, P. J. *J. Atmos. Chem.* **1999**, *32*, 375–395.
(73) Bard, A. J.; Parsons, R.; Jordan, J., *Standard Potentials in Aqueous Solution* 1985, Marcel Dekker, INC., New York, NY.
(74) Kaltsoyannis, N.; Plane, J. M. C. *Phys. Chem. Chem. Phys.* **2008**, *10*, 1723–1733.
(75) Bichsel, Y.; von Gunten, U. *Environ. Sci. Technol.* **1999**, *33*, 4040–4045.
(76) Carpenter, L. J.; Hopkins, J. R.; Jones, C. E.; Lewis, A. C.; Parthipan, R.; Wevill, D. J.; Poissant, L.; Pilote, M.; Constant, P. *Environ. Sci. Technol.* **2005**, *39*, 8812–8816.
(77) Martino, M.; Mills, G. P.; Woeltjen, J.; Liss, P. S. *Geophys. Res. Lett.* **2009**, *36*, L01609.

JP903486U